JOURNAL OF MATERIALS SCIENCE 32 (1997) 115–118

Comparison between the mechanical and dielectric strength distributions for hardened gypsum

YOSHINOBU NAKAMURA, MIKITO SUZUKI, NAOBUMI MOTOHIRA, AKIRA KISHIMOTO, HIROAKI YANAGIDA
Department of Applied Chemistry, Faculty of Engineering, The University of Tokyo, 7-3-1 Hongo, Bunkyo-ku, Tokyo 113, Japan

Hardened gypsum is chosen as a simple model of hardened cement materials and an analogy between the mechanical and dielectric strength distributions is investigated. Both of the strengths are evaluated in terms of Weibull statistics and a two-parameter Weibull function is adopted for both of the strength distributions. Both plots show good coincidence which is independent of the water content used during the mixing of hemihydrate gypsum powder for hardening. The hardened gypsum sheets made with 70 wt% of water, have mechanical and dielectric strength distributions that show two different behaviours in the Weibull plots, however, both the plots agree with each other. From our results, it is concluded that the mechanical strength distribution of hardened gypsum can be evaluated in terms of the dielectric strength distribution, which can be easily measured from a breakdown test.

1. Introduction

Chemical erosion of cement is known to introduce serious weak points to concrete. The diagnosis of this degradation generally requires, direct observation, which is wasteful from the technological view point. In order to prevent the sudden fracture of concrete, it has been reinforced. However this has resulted in the problem that the reliability of concrete or hardened cement material is now difficult to evaluate due to complicated textures, microstructures, and chemical compositions. If an easy and accurate method for the evaluation method of the strength or reliability of concrete could be established, then the reinforcement of concrete would not be necessary. Thus there is considerable interest in methods to evaluate the strength and reliability of concrete or hardened cement materials.

It is well known that large grains and pores are fracture sites in brittle materials and that mechanical strength strongly depends on the concrete microstructure since it determines the crack or pore size distributions [1]. The dielectric properties of materials are also microstructure dependent and an analogy between the mechanical and dielectric strength is possible. The authors have previously reported that the dielectric breakdown voltage in barium titanate ($BaTiO_3$), titanium dioxide (TiO_2) and other ceramic materials obeys the weakest link theory and have suggested an analogy between the mechanical and dielectric strength distributions [2–4]. In a porous material, the weak points for dielectric failure are suggested to be cracks or pores [5] which is analogous to the behaviour for mechanical strength.

In the present study, hardened gypsum is chosen as a simple model of a cement material, because its chemical composition is simple and its microstructure is easily controlled by varying the water–gypsum ratio in the mixing process. An analogy between the mechanical and dielectric strengths distribution of hardened gypsum is proposed and it is suggested that the determination of the mechanical strength distribution or reliability is possible by the use of dielectric breakdown tests.

2. Experimental procedure

Hemihydrate gypsum powder ($CaSO_4 \cdot 0.5H_2O$, Kojundo Kagaku Co., Ltd. purity $>99\%$) was sieved to obtain a sieve fraction of $\sim 100\,\mu m$. The starting powder was mixed with a prescribed amount of water for 2 min at 20 °C and put into a glass mould of $1 \times 20 \times 70$ mm size. The curing time was 24 h at 20 °C and hardened gypsum sheets were obtained. The end of the hydration reaction was confirmed by thermal gravimetric analysis (TGA) and no phases other than gypsum ($CaSO_4 \cdot 2H_2O$) was detected by X-ray diffraction (XRD) analysis after 24 h of curing. The prepared hardened body is cut into rectangular sheets of $1 \times 7 \times 20$ mm size and finished to a 0.6 mm thickness with a no. 2000 abrasive paper.

Both the mechanical and dielectric strength measurements were carried out at 20 °C. A three-point bending test (14 mm span and 21 MPa s^{-1} load speed) was employed for the estimation of the mechanical strength (σ_f) distribution. For the dielectric

0022–2461

breakdown test, silver electrodes with diffused edges (3 mm dia.) were evaporated onto both sides of the specimen to prevent edge-field concentration [4, 6]. The dielectric failure test was performed in silicon oil. A d.c. voltage was applied to the specimen and increased at the rate of 50 V s^{-1}. The breakdown field at which the electric current abruptly increased was regarded as the dielectric strength (E_b).

The experimentally measured mechanical and dielectric strengths were evaluated in terms of Weibull statistics [7]. The two-parameter Weibull function was adopted for the dielectric strength distribution.

$$P_1 = 1 - \exp[-(E_b/E_0)m_1 V_1] \quad (1)$$

The following equations, proposed by Yamashita *et al.* [2], were used for the comparison of the mechanical and dielectric strength distributions on the same scale.

$$P_1 = 1 - \exp[-(E_b/E)^{m_1}(E/E_0)^{m_1} V_1] \quad (2)$$

$$P_2 = 1 - \exp[-(\sigma_f/\sigma)^{m_2}(\sigma/\sigma_0)^{m_2} V_2] \quad (3)$$

where m_1 and m_2 are Weibull moduli, E and σ the average strengths of the mechanical fracture and dielectric breakdown, E_0 and σ_0 are scale parameters, and V_1 and V_2 are effective volumes for each strength. Using V_1 and E_0, the mean strength of Equation 2 is given by

$$E = E_0\Gamma(1 + 1/\dot{m}_1)/V^{-m_1} \quad (4)$$

where Γ is the gamma function. Equation 2 can be rewritten

$$P_1 = 1 - \exp[-(E_b/\bar{E})^{m_1}\Gamma(1 + 1/m_1)^{m_1}] \quad (5)$$

where we assume $E = \bar{E}$($\bar{E}$ is the mean dielectric strength for the test pieces). Equation 3 can also be rewritten

$$P_2 = 1 - \exp[-(\sigma_f/\bar{\sigma})^{m_2}\Gamma(1 + 1/m_2)^{m_2}] \quad (6)$$

where we also assume $\sigma = \bar{\sigma}$($\bar{\sigma}$ is the mean mechanical strength for the test pieces). With these equations, the comparison of both strength distributions by Weibull moduli becomes possible. Cumulative failure probabilities (P_1, P_2) were calculated using the mean rank method [4].

3. Results and discussion

The scanning electron microscope (SEM) view of the fracture cross-section of a hardened gypsum body fabricated by mixing with 60 wt % of water is shown in Fig. 1. Fine needle-like crystals of $CaSO_4 \cdot 2H_2O$ are observed in all the test pieces of hardened gypsum sheets and it was observed that the texture is independent of the water content during mixing. Fig. 2 shows the Weibull plots of mechanical and dielectric strength of hardened gypsum sheets that were made by mixing with 60 wt % of water. Both plots show good linearity, indicating that the scattering in each data set can be expressed by a single-mode Weibull distribution function and also that both mechanical and dielectric strength obey the weakest link theory. The Weibull plots of the mechanical and dielectric strengths of

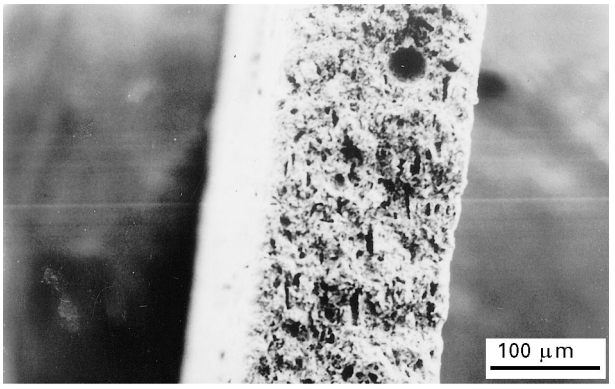

Figure 1 The SEM view of the fracture cross section of hardened gypsum body fabricated by mixing with 50 wt % of water.

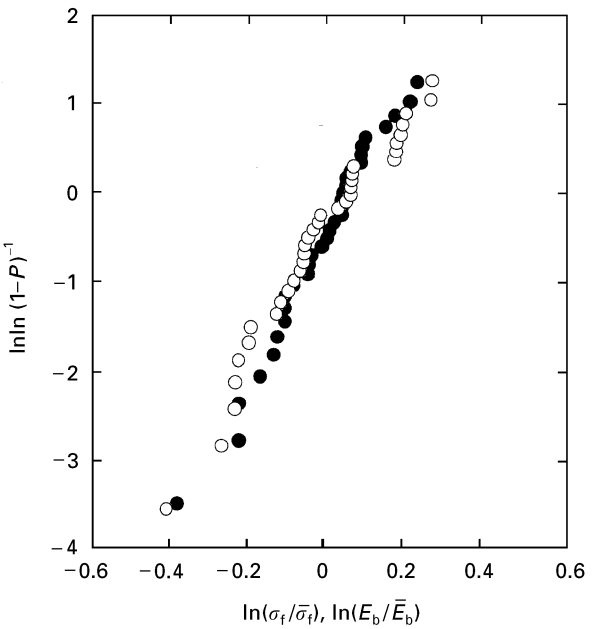

Figure 2 Weibull plots of mechanical and dielectric strength for hardened gypsum sheets made by mixing with 60 wt % of water. The (●) mechanical strength data produce an m value of 8.4 whilst the (○) dielectric strength data produce an m value of 7.2.

hardened gypsum sheets fabricated by mixing with 50 wt % of water are shown in Fig. 3. Similar results were obtained for the specimens which were made by mixing with 50, 55 or 60 wt % of water.

Fig. 4 shows the average mechanical and dielectric strengths of the hardened gypsum bodies made by mixing hemihydrate gypsum with prescribed amounts of water. Both strengths decrease gradually with an increase in water content during mixing and they show a rapid decrease at water contents of 60 wt % or higher. From SEM observation of a fracture cross-section produced by a three-point bending test, spherical pores of 50–150 μm diameter are observed and the number of these large pores in the hardened body increases with an increase in the water content during mixing. Since no difference was observed in the textures of needle-like $CaSO_4 \cdot 2H_2O$ crystals in the hardened bodies, the water content dependence of the mechanical and dielectric strengths is ascribed to the difference in size and distribution of the large spherical pores. Large pores in the hardened bodies were

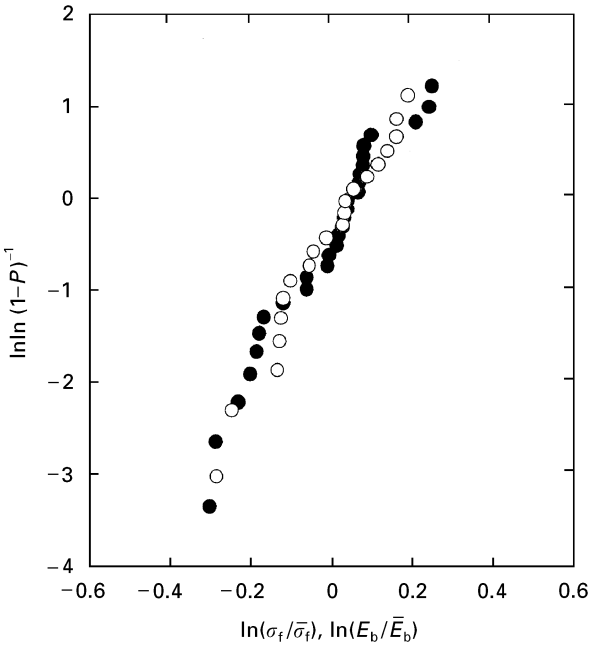

Figure 3 Weibull plots of mechanical and dielectric strength for hardened gypsum sheets made by mixing with 50 wt % of water. The (●) mechanical strength data produce an *m* value of 7.3 whilst the (○) dielectric strength data produce an *m* value of 7.8.

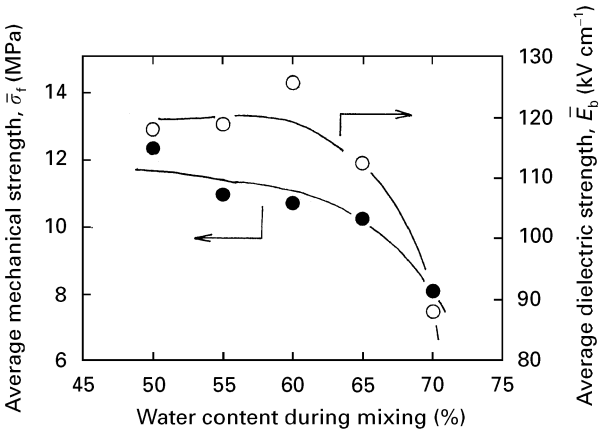

Figure 4 The relationship between the (●) average mechanical strength and (○) the average dielectric strength of hardened gypsum sheets and water content during mixing.

observed mainly in those test pieces which showed a relatively small value of the mechanical strength. It is suggested that they might be the origin of mechanical fracture. The relationship between the porosity and dielectric breakdown voltage has been studied by Beauchamp [5], and Murata *et al.* [8] and they have concluded that the dielectric breakdown voltage decreases with an increase in the porosity. A theoretical approach has also been employed in order to determine porosity effects on dielectric breakdown strength [9] in ceramic materials. The mechanical strength of hardened gypsum is also observed to depend on the porosity and it also decreases with an increase in the porosity. However, there is often an additional dependence on the shape of pores or surface flaws. In the present study, all the observable pores were spherical in shape and thus the effect of pore shape is not thought to be important.

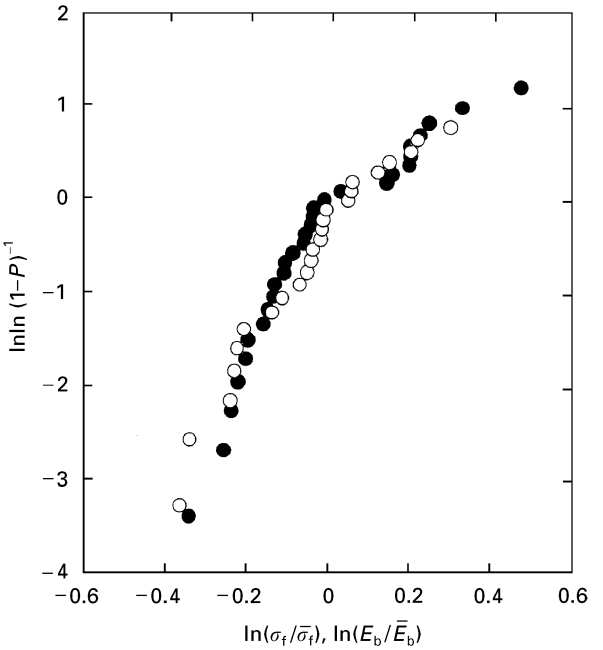

Figure 5 Weibull plots of mechanical and dielectric strength for hardened gypsum sheets made by mixing with 70 wt % of water. The (●) mechanical strength data produce an *m* value of 5.3 whilst the (○) dielectric strength data produce an *m* value of 5.6.

In Fig. 4, both the mechanical and dielectric strengths obey a similar rule and large pores that originated in the shrinkage of the hardening bodies would be a weak point for both the mechanical and dielectric failures. A drastic decrease in both the mechanical and the dielectric strengths are observed in the specimen with 70 wt % water content during mixing. Weibull plots obtained from the mechanical and dielectric strength data for hardened gypsum sheets which were fabricated by mixing with 70 wt % of water are shown in Fig. 5. Both plots bend at about the average strength and another fracture mode must be considered for both the mechanical and dielectric failures. However, both plots show good coincidence and an agreement between the distribution of weak points in both mechanical and dielectric failure is suggested even for the case of multi-mode fracture, which is often observed in brittle materials with complex texture.

Fig. 6(a–c) shows a typical breakdown track of a hardened gypsum body fabricated by mixing with 50 wt % of water. The inner surface of the track is melted and which is due to the generated Joule heat during the breakdown process. The origin of the dielectric failure cannot be specified from these figures. In Fig. 6(c), the breakdown track connects with a large spherical pore and this could be the origin of a fracture breakdown in the present case. A typical example of the current flow in the measuring circuit on the breakdown is shown in Fig. 7. The current suddenly increases at around the breakdown voltage and it is suggested that a sudden breakdown accompanied by an atmospheric spark discharge has occurred. The pore size in Fig. 6(c) is about 150 μm. The spark-breakdown gradient at a 150 μm gap is calculated to 85 kV per cm [10] which is in agreement with the

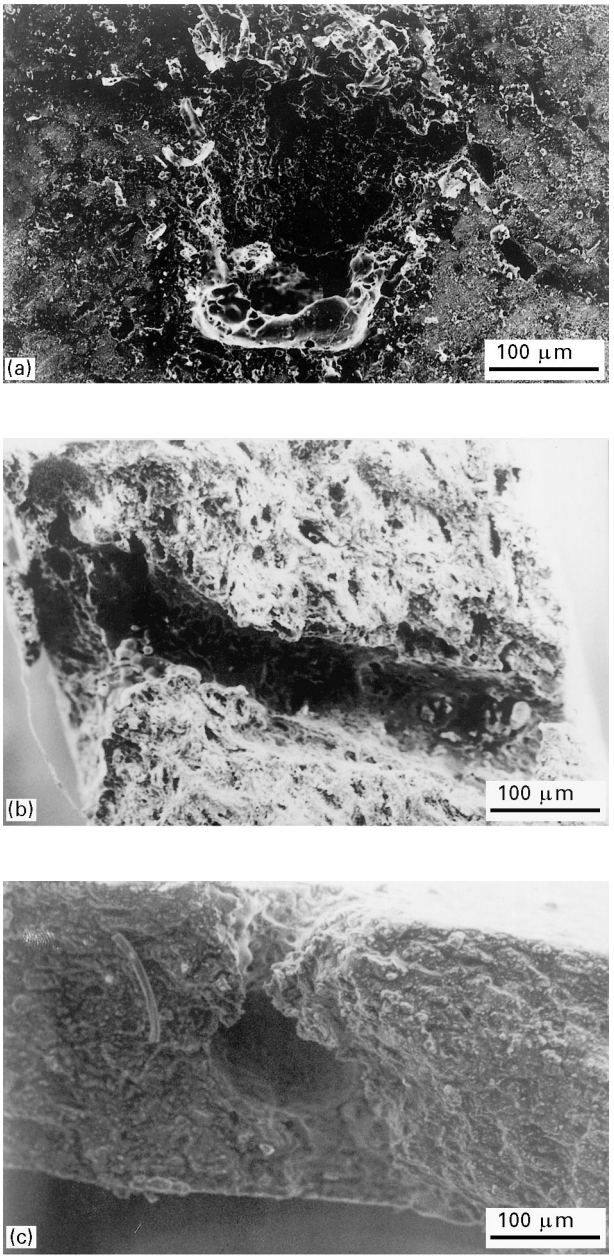

Figure 6 The SEM view of typical breakdown track of a hardened gypsum sheet fabricated by mixing 50 wt % of water: (a) surface, (b)(c) fracture cross-sections.

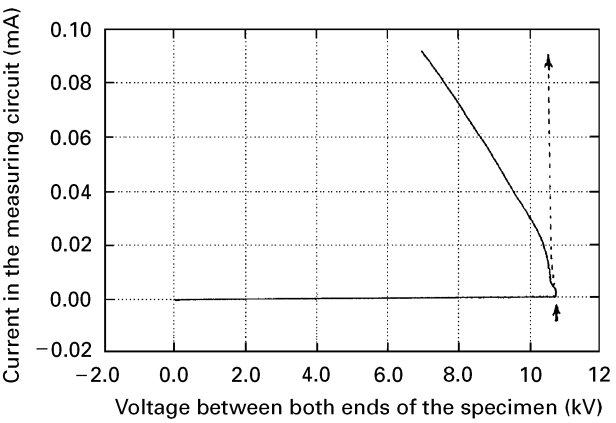

Figure 7 Typical current flow in the measuring circuit during the breakdown process. The horizontal axis is the voltage drop between both ends of the specimen, not the applied voltage. The breakdown voltage is indicated by the arrow. The practical current flow is shown as the broken line.

breakdown gradient of the hardened gypsum sheets fabricated by mixing with 50 wt % of water (80–140 kV per cm). If the origin for both mechanical and dielectric fracture is a large spherical pore, then there will be a coincidence of the Weibull plots for both the mechanical and dielectric failure tests. The results on the breakdown gradient of a pore in the present case would support our hypothesis, even if both the plots bend due to the operation of two different fracture modes for the mechanical or dielectric strengths.

4. Conclusion

The mechanical and dielectric strengths of hardened gypsum are measured and the distributions of both strengths are estimated by using Weibull statistics. When the water content during mixing is less than 60 wt %, the distributions of both strengths are expressed by a single-mode Weibull distribution function and they obey the weakest link theory. Both of the plots bend in the hardened gypsum sheets made by mixing with 70 wt % of water and their distributions are thought to be in good agreement. In some test pieces in the breakdown test, large spherical pores (50–150 μm in diameter) are observed at the centre of the breakdown track. The weak points for mechanical failure are suggested to be in common with dielectric failure. These weak points are the large spherical pores, which are generated by shrinkage of the hardened body during curing. From our results, it is suggested that the mechanical strength distribution of hardened gypsum can be evaluated in terms of the dielectric strength distribution, which can be easily obtained from a breakdown test.

References

1. W. DUCKWORTH, *J. Amer. Ceram. Soc.* **36** (1953) 68.
2. K. YAMASHITA, K. KOUMOTO and H. YANAGIDA, *ibid.* **67** (1984) C-67.
3. A. KISHIMOTO, K. KOUMOTO and H. YANAGIDA, *J. Mater. Sci.* **24** (1989) 698.
4. *Idem*, *J. Amer. Ceram. Soc.* **72** (1989) 1373.
5. E. K. BEAUCHAMP, *ibid.* **54** (1971) 484.
6. K. W. WAGNER, *Elect. Engr.* **4** (1922) 1034.
7. W. WEIBULL, *J. Appl. Mech.* **18** (1951) 293.
8. H. MURATA, S. C. CHOI, K. KOUMOTO and H. YANAGIDA, *J. Mater. Sci.* **20** (1985) 4507.
9. R. GERSON and T. C. MARSHALL, *J. Appl. Phys.* **30** (1959) 1650.
10. M. OHKI "High-Voltage Engineering (Jpn)" (Maki Publications, Tokyo, 1982).
11. J. D. COBINE "Gaseous Conductors" (Dover Publications, London, 1958).

Received 7 June 1995
and accepted 18 March 1996